Skeletal Muscle–Specific Activation of G_q Signaling Maintains Glucose Homeostasis

Derek B.J. Bone,[1] Jaroslawna Meister,[1] Jonas R. Knudsen,[2] Diptadip Dattaroy,[1] Amanda Cohen,[1] Regina Lee,[1] Huiyan Lu,[3] Daniel Metzger,[4] Thomas E. Jensen,[2] and Jürgen Wess[1]

Diabetes 2019;68:1341–1352 | https://doi.org/10.2337/db18-0796

Skeletal muscle (SKM) insulin resistance plays a central role in the pathogenesis of type 2 diabetes. Because G-protein–coupled receptors (GPCRs) represent excellent drug targets, we hypothesized that activation of specific functional classes of SKM GPCRs might lead to improved glucose homeostasis in type 2 diabetes. At present, little is known about the in vivo metabolic roles of the various distinct GPCR signaling pathways operative in SKM. In this study, we tested the hypothesis that selective activation of SKM G_q signaling can improve SKM glucose uptake and whole-body glucose homeostasis under physiological and pathophysiological conditions. Studies with transgenic mice expressing a G_q-linked designer GPCR selectively in SKM cells demonstrated that receptor-mediated activation of SKM G_q signaling greatly promoted glucose uptake into SKM and significantly improved glucose homeostasis in obese, glucose-intolerant mice. These beneficial metabolic effects required the activity of SKM AMPK. In contrast, obese mutant mice that lacked both $G\alpha_q$ and $G\alpha_{11}$ selectively in SKM showed severe deficits in glucose homeostasis. Moreover, GPCR-mediated activation of G_q signaling also stimulated glucose uptake in primary human SKM cells. Taken together, these findings strongly suggest that agents capable of enhancing SKM G_q signaling may prove useful as novel antidiabetic drugs.

Type 2 diabetes has emerged as a major threat to human health worldwide (1,2). The resistance of peripheral tissues, particularly of skeletal muscle (SKM), to the actions of insulin represents a key factor in the pathogenesis of type 2 diabetes (1–3).

G-protein–coupled receptors (GPCRs) are known to represent excellent drug targets (4). Like all other tissues, SKM, the largest insulin-sensitive organ in the body, expresses a considerable number of GPCRs that differ in their G-protein–coupling preferences (5). At present, little is known about the roles of SKM GPCRs in regulating glucose uptake and whole-body glucose homeostasis. A limited number of in vitro studies using cultured rat L6 SKM cells suggests that G_q-coupled receptors are able to promote glucose uptake in this SKM cell line (6,7). In contrast, a recent study showed that the G_q-coupled ET_B endothelin receptor inhibits glucose uptake in L6 myotubes (8). The reasons underlying these discrepant findings are unclear at present.

The potential in vivo roles of SKM G_q-coupled receptors remain unexplored. Work in this field has been complicated primarily by the fact that essentially all GPCRs are expressed in multiple tissues and cell types (5) and that most GPCRs show promiscuous G-protein–coupling properties (9). To overcome this obstacle, we started to use Designer Receptor Exclusively Activated by a Designer Drug (DREADD) technology (10,11). DREADDs represent mutant GPCRs that are no longer activated by any endogenous ligands but can be selectively activated by clozapine-*N*-oxide (CNO), a synthetic ligand that is otherwise pharmacologically inert (10,11). During the past few years, we and other investigators have successfully used DREADD technology to study the in vivo metabolic effects of activating distinct functional classes of GPCRs in several

[1]Molecular Signaling Section, Laboratory of Bioorganic Chemistry, National Institute of Diabetes and Digestive and Kidney Diseases, Bethesda, MD
[2]Section of Molecular Physiology, Department of Nutrition, Exercise and Sports, University of Copenhagen, Copenhagen, Denmark
[3]Mouse Transgenic Core Facility, National Institute of Diabetes and Digestive and Kidney Diseases, Bethesda, MD
[4]Institut de Génétique et de Biologie Moléculaire et Cellulaire, CNRS UMR 7104, INSERM U1258, Université de Strasbourg, Illkirch, France

Corresponding author: Jürgen Wess, jurgenw@niddk.nih.gov

Received 23 July 2018 and accepted 22 March 2019

This article contains Supplementary Data online at http://diabetes.diabetesjournals.org/lookup/suppl/doi:10.2337/db18-0796/-/DC1.

D.B.J.B. and J.M. are co–first authors.

metabolically relevant cell types, including pancreatic β-cells (12,13), hepatocytes (14–16), and adipocytes (17).

To elucidate the potential physiological roles of SKM G_q-linked GPCRs in vivo, we expressed a G_q-coupled DREADD (hM3Dq is M3Dq) (18) selectively in SKM cells of transgenic mice. In parallel, we also generated mutant mice that lacked $G\alpha_q/_{11}$ selectively in SKM. The outcome of systematic metabolic phenotyping studies strongly suggests that drugs able to stimulate SKM G_q-coupled receptors may become clinically useful for the treatment of type 2 diabetes.

RESEARCH DESIGN AND METHODS

All animal studies were approved by the National Institute of Diabetes and Digestive and Kidney Diseases (NIDDK)/National Institutes of Health (NIH) Animal Care and Use Committee.

Materials

CNO was obtained from the NIH as part of the Rapid Access to Investigative Drug Program funded by the National Institute of Neurological Disorders and Stroke. Sources of common chemicals, media, and commercial kits are provided in the text below or were from Sigma-Aldrich or Tocris Bioscience (oxytocin [OT] and L371,257).

Mouse Maintenance and Diet

Mice were fed ad libitum and kept on a 12-h light/dark cycle. Mice were maintained at room temperature (23°C) and consumed standard chow (15% kcal fat and energy density 3.1 kcal/g) (7022 NIH-07 diet; Envigo) or, where indicated, a high-fat diet (HFD) (50% kcal fat and energy density 5.5 kcal/g) (F3282; Bio-Serv).

Generation of SKM-M3Dq Mice

To generate mice that selectively express the G_q-coupled DREADD M3Dq in SKM (SKM-M3Dq mice), we first inserted the hemagglutinin (HA)-hM3Dq-p2A-mCitrine sequence (plasmid source: Dr. Bryan Roth, University of North Carolina at Chapel Hill, Chapel Hill, NC) into the pHSAvpSV40pA plasmid (19). In this construct, expression of the M3Dq designer receptor is under the transcription control of the human α-skeletal actin (HSA) promoter. The linearized HSA-M3Dq-p2a-mCitrine plasmid was microinjected into the pronuclei of fertilized ova from C57BL/6NTac mice (Taconic Farms, Germantown, NY) using standard transgenic techniques. Mice harboring the HSA-M3Dq transgene were identified via PCR of genomic tail DNA. We identified a mouse line that selectively expressed the HSA-M3Dq transgene in SKM (see text for details). For simplicity, we refer to these mice as SKM-M3Dq mice throughout the manuscript. Hemizygous SKM-M3Dq mice were crossbred with wild-type (WT) C57BL/6NTac mice, and littermates not carrying the M3Dq allele served as control animals (genotyping information is available upon request).

Generation of SKM-M3Dq-AMPK-DN Mice

The generation of MCK-AMPK–dominant-negative (DN) mice has been described previously (genetic background C57BL/6) (20). SKM-M3Dq mice were crossed with MCK-AMPK-DN mice to generate SKM-M3Dq-AMPK-DN mice (genotyping information is available upon request).

Generation of Mice Selectively Lacking $G\alpha_q/_{11}$ in SKM

$Ga_q^{flox/flox}Ga_{11}{}^{-/-}$ mice (21) were crossed with HSA-Cre (ER^{T2}) mice (22) (genetic background of both strains: C57BL/6) to produce HSA-Cre(ER^{T2}) $Ga_q^{flox/+}Ga_{11}{}^{-/+}$ offspring. These mice were backcrossed to $Ga_q^{flox/flox}Ga_{11}{}^{-/-}$ mice line to generate HSA-Cre(ER^{T2}) $Ga_q^{flox/flox}Ga_{11}{}^{-/-}$ mice used for experimentation. To induce Cre recombinase activity, HSA-Cre(ER^{T2}) $Ga_q^{flox/flox}$ mice were injected i.p. with 2 mg of tamoxifen dissolved in corn oil for 5 consecutive days (22), leading to the selective deletion of *Gaq* in SKM. $Ga_q^{flox/flox}Ga_{11}{}^{-/-}$ mice littermates lacking the Cre(ER^{T2}) transgene also received tamoxifen and served as control animals (genotyping information is available upon request).

Intraperitoneal Glucose Tolerance Test

Mice were fasted overnight for 14–16 h and then injected i.p. with normal saline containing 2 g/kg glucose in the presence or absence of 1 mg/kg CNO. Blood glucose concentrations were determined with a Bayer Contour glucometer using blood collected from the tail vein immediately before and at defined time points after i.p. injections.

Insulin Tolerance Test

Mice were fasted for 5 h starting at 9 A.M. and then injected i.p. with human insulin (0.75 units/kg or 1.5 units/kg, as indicated; Humulin R; Eli Lilly and Company) in the presence or absence of 1 mg/kg CNO. Blood glucose levels were determined in the same fashion as described in the previous paragraph.

Glucose-Stimulated Insulin Secretion

Mice were fasted overnight for 14–16 h and then injected i.p. with normal saline containing 2 g/kg glucose in the presence or absence of 1 mg/kg CNO. Plasma insulin concentrations were determined using blood collected from the tail vein immediately before and at defined time points after i.p. injections. Blood was collected into heparinized capillary tubes, and plasma was isolated via centrifugation. Plasma insulin levels were determined with a commercial ELISA kit (Crystal Chem).

In Vivo [^{14}C]2-Deoxyglucose Uptake

To measure glucose uptake into individual tissues in vivo, mice were fasted overnight for 14–16 h and then injected i.p. with saline containing 2 g/kg glucose and 10 μCi of [^{14}C]2-deoxyglucose ([^{14}C]2-DG) (PerkinElmer), in the presence or absence of 1 mg/kg CNO. Mice were sacrificed 2 h later, and SKM and other tissues were harvested. Tissue content of [1-^{14}C]2-DG-6-phosphate was determined as a measure of SKM glucose uptake as described previously (23).

Measurement of M3Dq RNA Expression in SKM-M3Dq Mice via Quantitative RT-PCR

WT and SKM-M3Dq mice were sacrificed, and tissues were dissected and snap-frozen in liquid nitrogen. Tissue biopsies were homogenized in TRIzol reagent (Thermo Fisher Scientific), and total RNA was isolated. cDNA was generated from total RNA using the Superscript III RT kit with oligo(dT) primers (Thermo Fisher Scientific). Subsequently, cDNA was screened for the presence of M3Dq DNA using standard PCR techniques. The presence of the transgene was detected by using the following primers: forward, 5′-AGAAGAACGGCATCAAGGTG-3′ and reverse, 5′-GAACTCCAGCAGGACCATGT-3′ (amplicon size: 200 bp).

Radioligand Binding Studies

Crude membranes were prepared from quadriceps muscle of WT and SKM-M3Dq mice, as described previously (24). [^{3}H]-*N*-methylscopolamine ([^{3}H]-NMS)–saturating (70 Ci/mmol; PerkinElmer) binding studies were carried out as described (12). Briefly, 60 μg of membrane protein was incubated with increasing concentrations of [^{3}H]-NMS (1–50 nmol/L) in a 0.25 mL volume at room temperature for 3 h. Binding mixtures were then filtered over GF/B filters presoaked in 0.3% polyethyleneimine (Brandel). Nonspecific binding was determined as binding in the presence of atropine (10 μmol/L). Radioactivity was counted using standard liquid scintillation techniques.

CNO Administration via the Drinking Water

In a subset of experiments, CNO was administered continuously for 7 days by mixing CNO into the mouse drinking water at a concentration of 0.25 mg/mL, as described previously (13).

Adenoviruses

The adenovirus coding for M3Dq (titer: 1.2×10^{12} transducing units/mL) was generated by the University of North Carolina at Chapel Hill Vector Core (director Dr. D. Dismuke, Chapel Hill, NC). The human M3Dq coding sequence (18) was inserted into the pShuttle-CMV-IRES-mCitrine vector. The adenovirus coding for GFP (titer: 3.2×10^{11} IFU/mL) was a gift from the laboratory of Dr. M. Montminy (Salk Institute for Biological Studies, La Jolla, CA).

Culture of L6-GLUT4myc Cells and Transfection

L6-GLUT4myc cells (25) were obtained from Kerafast and cultured according to the provider's specifications. For experiments, L6-GLUT4myc myoblasts were plated at a concentration of 4×10^4 cells/mL in 24-well plates. On the following day, the growth medium was replaced with antibiotic-free α-minimum essential medium Eagle (α-MEM) containing 20% FBS, and cells were transfected with a plasmid coding for hM3Dq (pcDNA3-HA-hM3Dq-p2A-mCitrine; University of North Carolina at Chapel Hill Vector Core) or pCMV-GFP (plasmid #11153; Addgene) using Lipofectamine 3000 (Thermo Fisher Scientific). About 24 h later, the medium was replaced with the original complete growth medium (α-MEM). Experiments were performed on the second day after transfection following serum starvation of cells for 3 h.

[^{3}H]2-DG Uptake Measurements With L6-GLUT4myc Cells

L6-GLUT4myc cells were cultured as described in the previous paragraph. The uptake of [^{3}H]2-DG (8 Ci/mmol; PerkinElmer) by transfected L6-GLUT4myc cells was measured as described previously (26). Thirty minutes after the addition of pharmacological inhibitors, cells were treated with 10 μmol/L CNO for 60 min, followed by the addition of 100 nmol/L insulin for an additional 20 min (where indicated). Incubations with insulin alone (100 nmol/L) were carried out for 20 min. Specific uptake in the absence of CNO and/or insulin was defined as basal uptake (100%). All data were expressed as percent of basal uptake. Experiments were performed in triplicate.

Functional Studies With Primary Human SKM Cells

Primary human SKM myoblasts (HSMMs; Lonza) were cultured according to the provider's specifications. Briefly, HSMMs were seeded into 12-well plates at 8×10^4 cells/well. Upon reaching 80% confluence, HSMMs were differentiated into myotubes for 4 to 5 days in DMEM/F12 medium containing 2% horse serum. Prior to glucose uptake experiments, cells were serum starved in DMEM/F12 medium for 3 h, followed by treatment with OT for 1 h at 37°C. Where indicated, pharmacological inhibitors were added during the last 30 or 60 min (compound C; L-371,257) of serum starvation.

In a separate set of experiments, the M3Dq construct was expressed in HSMMs by using an M3Dq-encoding adenovirus. For control purposes, HSMMs were transduced with an adenovirus coding for GFP. Adenoviruses were added to the growth medium at a multiplicity of infection of 250 3 days after the start of differentiation process. On the following day, the medium was replaced with fresh differentiation medium. Glucose uptake studies were performed with transduced cells 2 days after virus addition.

[^{3}H]2-DG uptake studies were performed in the same fashion as described for L6-GLUT4myc cells (see previous paragraph), except that the [^{3}H]2-DG incubation time was increased to 15 min. All experiments were carried out in duplicate.

GLUT4 Cell Surface Expression

Detection of cell surface GLUT4 expression in L6-GLUT4-myc cells was based on a previously described method (25) modified for flow cytometry (27). L6-GLUT4myc cells were seeded at a density of 1.25×10^6 cells in 10-cm dishes. On the following day, cells were transfected with the HA-hM3Dq construct (18) as described above. Two days later, cells were serum starved for 2.5 h and then lifted from the plates using Cell Stripper reagent (Corning). Cells were resuspended in serum-free basal α-MEM at a concentration of 1×10^6 cells/mL. Subsequently, 500 μL of cell

suspension was added to flow cytometry tubes (BD Biosciences) and incubated at 37°C for 30 min. Any inhibitors used were added during this incubation step. Cells were treated with 10 μmol/L CNO for 1 h at 37°C and, if required, for an additional 20 min with 100 nmol/L insulin. Incubations were terminated by centrifugation of cells at 220*g* for 5 min. Cells were then resuspended in ice-cold 3% paraformaldehyde in PBS and incubated on ice for 10 min. Sodium azide (15 μmol/L) was added to the cells prior to storage at 4°C until further analysis.

In order to detect cell surface GLUT4 (mycGLUT4), fixed cells were washed in incubation buffer (0.5% BSA in PBS) and incubated with antimyc (mycGLUT4) and anti-HA (HA-M3Dq) primary antibodies for 1 h at room temperature. Cells were then washed and incubated with fluorescent secondary antibodies for 30 min at room temperature protected from light. After this incubation step, cells were resuspended in incubation buffer and analyzed using a BD FACSCalibur Flow Cytometer (BD Biosciences). The mean fluorescence intensity caused by the myc tag in the absence of stimulating drugs was defined as basal GLUT4 cell surface expression. Drug effects were expressed as increases in GLUT4 expression in percent above basal expression. In all experiments, 1×10^4 cells were counted per replicate. All experiments were performed in duplicate.

The following primary antibodies were used: anti–HA-tag rabbit monoclonal antibody (mAb) (#3724; Cell Signaling Technology) and anti–myc-tag mouse mAb (#2276; Cell Signaling Technology). The following secondary antibodies were used: anti-rabbit IgG (Alexa Fluor 488 Conjugate, #4412; Cell Signaling Technology) and chicken anti-mouse IgG (Alexa Fluor 647, #A-21463; Invitrogen/Thermo Fisher Scientific).

Western Blotting Experiments

Control and HSA-M3Dq transgenic mice that had been fasted for 5 h were injected i.p. with insulin (0.75 IU/kg) and CNO (1 mg/kg) dissolved in normal saline. Twenty minutes later, mice were sacrificed, and gastrocnemius muscles were isolated and snap-frozen in liquid nitrogen for Western blotting studies. Immunoblotting studies were performed using standard procedures. Immunoreactive proteins were visualized using SuperSignal West Dura Extended Duration Substrate (Thermo Fisher Scientific) on the c600 Imaging System (Azure Biosystems) and quantified using ImageJ (NIH). Protein expression levels were normalized to the amount of loaded GAPDH (control).

HSMMs were cultured as described under FUNCTIONAL STUDIES WITH PRIMARY HUMAN SKM CELLS. Prior to OT (1 μmol/L) treatment, cells were serum starved in DMEM/F12 medium for 5 h. In a separate set of experiments, M3Dq or GFP (controls) were expressed in HSMMs via adenovirus-mediated gene transfer (see above). Prior to incubation with CNO (10 μmol/L), transduced myotubes were serum starved in DMEM/F12 medium for 5 h. Western blotting studies were performed using standard procedures (see previous paragraph).

The following primary antibodies were used: total AMPK rabbit antibody (#2532S; Cell Signaling Technology), phospho AMPK (pAMPK) rabbit mAb (#9272S; Cell Signaling Technology), pAKT (S473) rabbit mAb (#3787S; Cell Signaling Technology), total AKT rabbit mAb (#9272S; Cell Signaling Technology), and GAPDH rabbit mAb (HRP-linked, #3683; Cell Signaling Technology). Anti-rabbit IgG (HRP-linked) from Cell Signaling Technology (#7074S) was used as the secondary antibody.

Statistical Analysis

Data are expressed as means ± SEM for the indicated number of observations. The SPSSs used are indicated in the figure legends. Statistical differences were determined using a two-tailed *t* test or one-way ANOVA followed by Tukey post hoc test, as appropriate. A P value of <0.05 was considered significant.

RESULTS AND DISCUSSION

Expression and Activity of a G_q DREADD in Cultured SKM Cells

We first examined whether CNO activation of a G_q-linked DREADD (M3Dq) (18) expressed in cultured SKM cells was able to promote glucose uptake. We transiently expressed the M3Dq DREADD in L6-GLUT4myc myoblasts that stably express a myc-tagged version of GLUT4 (25). To study M3Dq expression levels, we carried out saturation binding assays using the muscarinic antagonist [^{3}H]-NMS as a radioligand (12). This analysis detected 792 ± 81 fmol/mg protein of M3Dq receptors in the M3Dq-transfected cells (means ± SEM; n = 3). No specific [^{3}H]-NMS binding sites were detected in L6-GLUT4myc control cells expressing GFP.

CNO treatment of M3Dq-L6-GLUT4myc cells resulted in a pronounced increase in inositol monophosphate accumulation, consistent with the activation of G_q-type G-proteins (Supplementary Fig. 1). This response was absent in control cells expressing GFP (Supplementary Fig. 1).

CNO (10 μmol/L) treatment of M3Dq-L6-GLUT4myc cells also led to a significant increase in the uptake of [^{3}H]2-DG (Fig. 1*A*). This CNO effect was not observed with GFP-L6-GLUT4myc control cells (Fig. 1*A*). The magnitude of the CNO response displayed by the M3Dq-expressing cells was not significantly different from that obtained after simulation of M3Dq-L6-GLUT4myc or control cells with insulin (100 nmol/L) (Fig. 1*A*). CNO (10 μmol/L) was also able to enhance insulin-induced 2-DG uptake over a wide range of insulin concentrations (Fig. 1*B*).

To test whether the CNO-mediated increase in 2-DG uptake in M3Dq-L6GLUT4myc cells was associated with an increase in GLUT4 translocation to the cell surface, we took advantage of the extracellular myc-tag fused to GLUT4 expressed by L6-GLUT4myc cells and the HA-tag attached to the extracellular N-terminus of the M3Dq construct. These two epitope tags enabled us to use

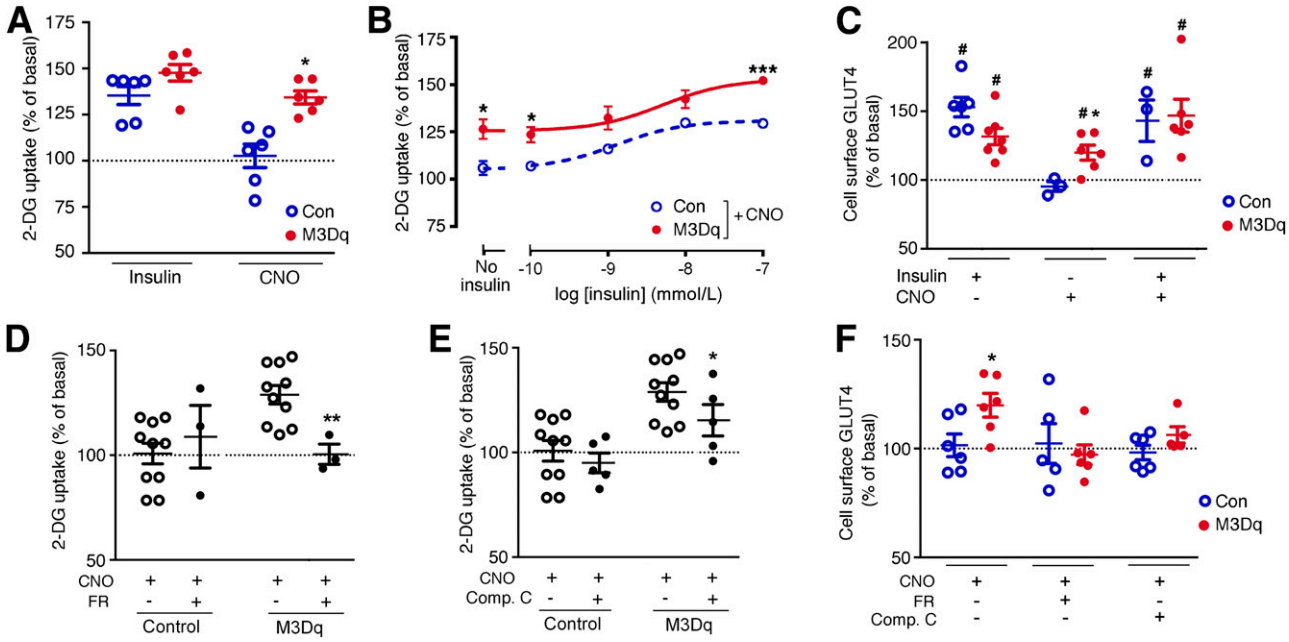

Figure 1—Activation of a G_q-linked designer GPCR (M3Dq) promotes glucose uptake and GLUT4 translocation in vitro. *A–F*: Functional studies were carried out with L6-GLUT4myc myoblasts expressing either M3Dq or GFP (control [Con]). *A* and *B*: [^{3}H]2-DG uptake was studied following incubation of L6-GLUT4myc cells with either insulin (100 nmol/L) or CNO (10 μmol/L), as described in detail in RESEARCH DESIGN AND METHODS. In *B*, CNO (10 μmol/L) stimulation of [^{3}H]2-DG uptake was measured in the presence of increasing insulin concentrations. *C*: CNO (10 μmol/L) promotes the translocation of GLUT4 to the cell surface of M3Dq-L6GLUT4myc myoblasts. GLUT4 cell surface expression was determined using a FACS-based approach, as described in RESEARCH DESIGN AND METHODS. *D*: CNO-induced (10 μmol/L) stimulation of [^{3}H]2-DG uptake in M3Dq-L6-GLUT4myc myoblasts is completely abolished by FR900359 (FR; 1 μmol/L), a selective inhibitor of $G_{q/11}$. *E*: CNO-mediated (10 μmol/L) enhancement of [^{3}H]2-DG uptake in M3Dq-L6GLUT4myc myoblasts is greatly reduced in the presence of compound C (Comp. C; 10 μmol/L), an AMPK inhibitor. *F*: CNO-induced (10 μmol/L) translocation of GLUT4 to the cell surface of M3Dq-L6GLUT4myc myoblasts is abolished in the presence of FR (1 μmol/L) or Comp. C (10 μmol/L). Data are expressed as means ± SEM of six (*A–C* and *F*), three (*D*), or seven (*E*) independent experiments, each performed in duplicate or triplicate. All responses were expressed relative to baseline responses (set equal to 100%) obtained in the absence of drugs. Basal [^{3}H]2-DG uptake values were similar ($P = 0.13$) between M3Dq-expressing and GFP control cells (62,375 ± 1,531 and 73,786 ± 5,862 dpm/mg protein, respectively). *$P < 0.05$, **$P < 0.01$, ***$P < 0.001$ vs. control (Student *t* test); #$P < 0.05$ as compared with baseline (100%; no drug treatment; one-sample *t* test).

FACS technology to measure cell surface GLUT4 expression levels in response to insulin (100 nmol/L) and CNO (10 μmol/L) (see RESEARCH DESIGN AND METHODS for details). Insulin treatment caused a significant increase in GLUT4 cell surface translocation in M3Dq-L6-GLUT4myc cells and in control cells that did not express the M3Dq construct (Fig. 1*C*). In line with the 2-DG uptake data, CNO treatment also caused a significant increase in cell surface GLUT4 expression in M3Dq-L6-GLUT4myc cells, but not in control cells (Fig. 1*C*). The treatment of M3Dq-L6-GLUT4myc cells with a combination of insulin (100 nmol/L) and CNO (10 μmol/L) did not lead to a further enhancement of insulin-induced GLUT4 translocation (Fig. 1*C*), in contrast to the 2-DG uptake data (Fig. 1*B*). One possible reason for this discrepancy is that 2-DG uptake was measured in a cumulative fashion, while the GLUT4 translocation experiment captured the amount of GLUT4 protein present in the plasma membrane at a single time point. Moreover, it has been shown that GLUT4 translocation and activation are separate events (28).

To confirm that the M3Dq-dependent increases in 2-DG uptake and GLUT4 translocation in M3Dq-L6-GLUT4myc cells were indeed mediated by G-proteins of the G_q family, we used FR900359 (alternative name UBO-QIC), a selective inhibitor of $G_{q/11}$ signaling (29). Consistent with the predicted coupling properties of the M3Dq DREADD, M3Dq-mediated increases in 2-DG uptake and GLUT4 cell surface expression in M3Dq-L6-GLUT4myc cells were completely blocked by FR900359 (1 μmol/L) (Fig. 1*D* and *F*).

Previous work has demonstrated that enhanced G_q signaling can lead to the activation of AMPK in different cell types including SKM cells (6,30,31). We found that treatment of M3Dq-L6-GLUT4myc cells with compound C (10 μmol/L), an inhibitor of AMPK, greatly reduced both CNO-induced 2-DG uptake and GLUT4 translocation (Fig. 1*E* and *F*).

Taken together, these in vitro studies suggest that activation of a G_q-linked designer GPCR in cultured SKM cells leads to G_q- and AMPK-dependent increases in glucose uptake and GLUT4 translocation.

Generation of a Transgenic Mouse Line Selectively Expressing the M3Dq DREADD in SKM

To explore the in vivo metabolic effects caused by selective stimulation of a G_q-linked GPCR in SKM, we generated

a transgenic mouse line in which the expression of M3Dq was under the transcriptional control of the HSA promoter (see RESEARCH DESIGN AND METHODS for details). RT-PCR studies confirmed that the M3Dq designer receptor was selectively expressed in mouse SKM (Supplementary Fig. 2*A*). In the following, we refer to these newly generated transgenic mice as SKM-M3Dq mice. Radioligand binding studies detected 90 ± 21 fmol of [^{3}H]-NMS binding sites/mg protein in mouse SKM (quadriceps muscle membranes) of SKM-M3Dq mice (Supplementary Fig. 2*B*). [^{3}H]-NMS also labeled a small population of endogenous muscarinic receptors in SKM of WT littermates (29 ± 5 fmol/mg protein) (Supplementary Fig. 2*B*), suggesting that the M3Dq designer receptor is expressed at a density of ~60 fmol/mg protein in SKM of SKM-M3Dq transgenic mice. This value is within the range at which many endogenous GPCRs are expressed in peripheral tissues including SKM. The fact that the M3Dq receptor was expressed at considerably lower levels in mouse SKM than in cultured L6-GLUT4myc cells (see above) may explain some of the differences that we observed between the in vitro and in vivo experiments.

Activation of M3Dq Signaling in SKM Improves Whole-Body Glucose Homeostasis

SKM-M3Dq mice and their WT littermates did not differ in body weight, glycemia, and plasma insulin levels (Supplementary Fig. 3). Likewise, both groups of mice showed similar blood glucose excursions in an i.p. glucose tolerance test (IGTT) in the absence of CNO (Fig. 2*A*). Strikingly, coinjection (i.p.) of glucose (2 g/kg) with CNO (1 mg/kg) resulted in greatly improved glucose tolerance in SKM-M3Dq mice, as compared with their WT littermates (Fig. 2*B*). We also injected SKM-M3Dq and WT mice with saline or CNO (1 mg/kg i.p.) alone. The SKM-M3Dq mice, like the WT mice, showed a significant increase in blood glucose levels during the first 30 min after saline injection, most likely due an injection-induced stress response. Interestingly, this effect was absent in CNO-injected SKM-M3Dq mice (Supplementary Fig. 4), suggesting that CNO-mediated activation of SKM M3Dq caused a decrease in blood glucose levels that counteracted the stress-induced hyperglycemic response.

An insulin tolerance test (ITT) showed that SKM-M3Dq mice and their WT littermates showed comparable decreases in blood glucose levels in the absence of CNO (Fig. 2*C*). In contrast, coinjection of SKM-M3Dq mice with insulin (1.5 units/kg i.p.) plus CNO (1 mg/kg i.p.) led to a significant improvement in insulin sensitivity, as compared with WT littermates treated in the same fashion (Fig. 2*D*). Coinjection (i.p.) of glucose (2 g/kg) with CNO (1 mg/kg) caused comparable increases in plasma insulin levels in SKM-M3Dq mice and control littermates (Fig. 2*E*), indicating that pancreatic insulin release remained unaffected by activation of the M3Dq designer receptor in SKM.

To test the hypothesis that the CNO-induced improvement in glucose tolerance observed with SKM-M3Dq mice was the result of increased glucose uptake into SKM, we coinjected (i.p.) SKM-M3Dq mice and their WT littermates with glucose (2 g/kg) containing 10 μCi of [1-^{14}C]2-DG (23). Accumulation of the [^{14}C]2-DG metabolite, 2-DG-6-phosphate, was determined as a measure of glucose uptake in various tissues. As predicted, CNO (1 mg/kg i.p.) treatment of SKM-M3Dq mice dramatically increased 2-DG uptake into SKM tissues (quadriceps, gastrocnemius, and triceps muscles) (Fig. 3*A–C*). No such effect was observed with non-SKM tissues (Fig. 3*D–F*) or with SKM tissues prepared from WT mice (Fig. 3*A–C*).

Taken together, the in vivo data strongly support the concept that selective activation of a G_q-linked designer receptor in SKM of transgenic mice greatly improves glucose homeostasis by selectively enhancing glucose uptake into SKM.

SKM AMPK Is Required for M3Dq-Mediated Improvements in Glucose Homeostasis In Vivo

Because inhibition of AMPK greatly reduced M3Dq-mediated glucose uptake in cultured SKM cells (Fig. 1*E*), we next studied whether AMPK played a similar role in mediating the beneficial metabolic effects caused by activation of SKM M3Dq receptors in vivo. We crossed SKM-M3Dq mice with SKM-specific AMPK-DN mice (20) to produce a new transgenic mouse line coexpressing M3Dq and AMPK-DN in SKM (SKM-M3Dq-AMPK-DN mice) (see RESEARCH DESIGN AND METHODS for details). As already shown in Fig. 2*B*, coinjection (i.p.) of glucose (2 g/kg) with CNO (1 mg/kg) resulted in significantly improved glucose tolerance in SKM-M3Dq mice, as compared with WT littermates (Fig. 4*A*). Strikingly, this beneficial CNO effect was completely abolished in SKM-M3Dq-AMPK-DN mice (Fig. 4*A*). This observation strongly supports the concept that G_q-mediated activation of SKM AMPK also plays a key role in improving glucose tolerance in vivo. Somewhat surprisingly, CNO-treated (1 mg/kg i.p.) SKM-M3Dq-AMPK-DN showed similar whole-body insulin tolerance as CNO-treated SKM-M3Dq mice (Fig. 4*B*), suggesting that additional, non-AMPK–dependent pathways contribute to M3Dq-mediated improvements in insulin sensitivity. Additional possibilities are that glucose engages AMPK more effectively than insulin or that AMPK activities were different at the beginning of the ITT versus IGTT experiments (note that mice were fasted for a much longer time for the IGTT studies).

In the SKM-M3Dq-AMPK-DN mice, the AMPK-DN construct was expressed under the transcriptional control of the MCK promoter that is also active in cardiac muscle (20), raising the possibility that inactivation of AMPK in cardiac muscle may also contribute to the phenotypes displayed by the SKM-M3Dq-AMPK-DN mice. However, a recent study demonstrated that inactivation of AMPK in cardiac muscle has no significant effect on myocardial energy metabolism (32), suggesting that it is unlikely that impairment of myocardial AMPK function makes a significant contribution to the metabolic phenotypes displayed by the SKM-M3Dq-AMPK-DN mice.

To confirm that activation of the M3Dq designer receptor in SKM of SKM-M3Dq mutant mice promoted the formation

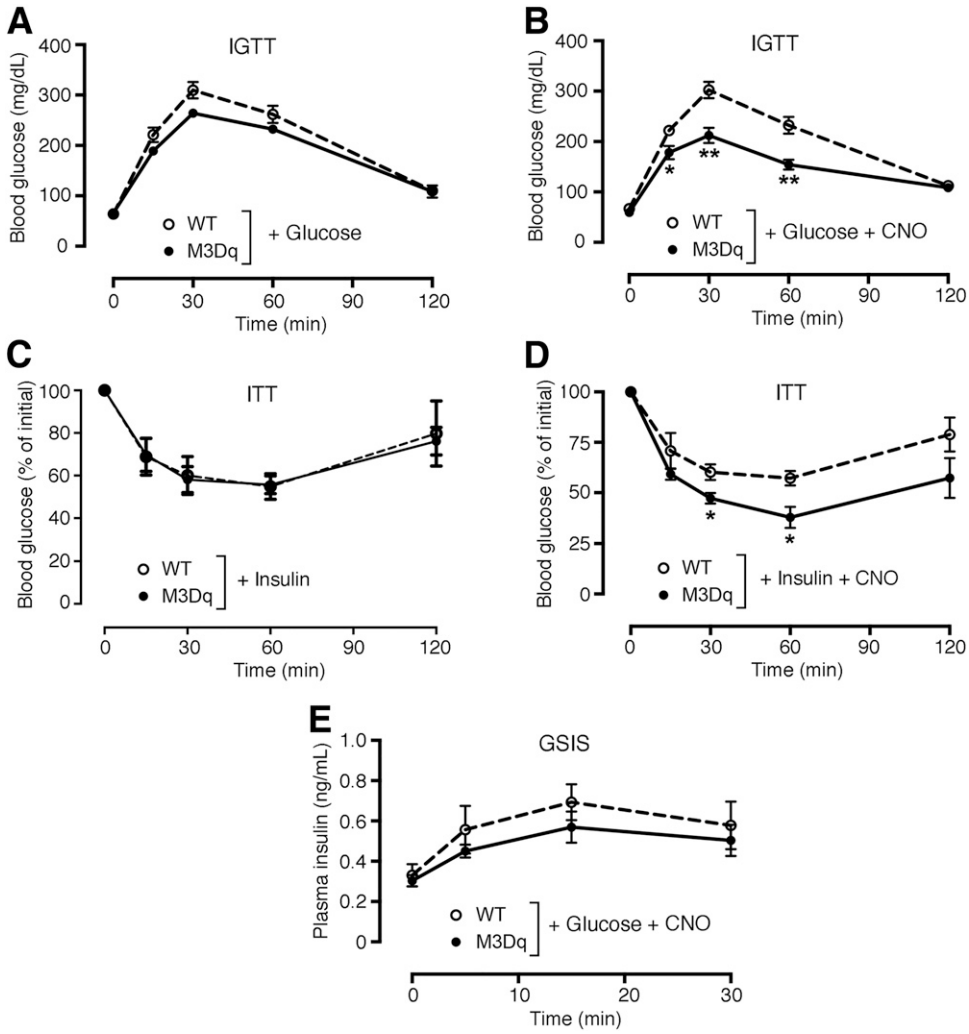

Figure 2—Selective activation of M3Dq in SKM improves glucose tolerance and insulin sensitivity in mice in vivo. *A* and *B*: IGTT. SKM-M3Dq mice (M3Dq) and WT control littermates were injected with glucose (2 g/kg i.p.) (*A*) or glucose (2 g/kg i.p.) plus CNO (1 mg/kg i.p.) (*B*). *C* and *D*: ITT. SKM-M3Dq mice (M3Dq) and WT control littermates were injected with insulin (1.5 units/kg i.p.) (*C*) or insulin (1.5 units/kg i.p.) plus CNO (1 mg/kg i.p.) (*D*). *E*: Glucose-stimulated insulin secretion (GSIS). SKM-M3Dq mice (M3Dq) and WT control littermates were injected with glucose (2 g/kg i.p.) plus CNO (1 mg/kg i.p.). Data are given as means ± SEM ($n = 5$ or 6 mice/group). $^*P < 0.05$, $^{**}P < 0.01$ vs. WT (Student *t* test).

of pAMPK, we coinjected HSA-M3Dq transgenic mice and their control littermates with insulin (0.75 IU/kg i.p.) and CNO (1 mg/kg i.p.). Western blotting studies showed that this treatment led to a significant increase in AMPK phosphorylation in SKM (gastrocnemius muscle) of the DREADD mutant mice, as compared with SKM prepared from control littermates (Supplementary Fig. 5*A* and *B*). Under the same experimental conditions, we observed a clear trend toward reduced SKM AKT phosphorylation (pAKT [S473]) in the mutant animals (Supplementary Fig. 5*C* and *D*).

Receptor-Mediated SKM G_q Signaling Improves Glucose Homeostasis in a Mouse Model of Type 2 Diabetes

Because acute activation of G_q signaling in SKM resulted in dramatic improvements in glucose tolerance and insulin sensitivity in lean mice, we next examined whether activation of this pathway might prove useful to overcome the metabolic deficits displayed by obese mice, including glucose intolerance and insulin resistance.

We maintained SKM-M3Dq mice and their WT littermates on an HFD for 8 weeks. After this period, both groups of mice displayed a similar degree of body weight gain, fasting hyperglycemia, and glucose intolerance (Supplementary Fig. 6). HFD SKM-M3Dq mice and their WT littermates were then treated with CNO for 1 week by adding CNO to the drinking water (0.25 mg CNO/mL) (13). CNO treatment of SKM-M3Dq mice, but not of control mice, led to a dramatic reduction in fasting blood glucose and plasma insulin levels (Fig. 5*A*), indicative of a pronounced increase in peripheral insulin sensitivity. Fasting blood glucose levels measured after CNO treatment of HFD SKM-M3Dq mice were similar to those determined in control mice maintained on normal mouse chow (Supplementary Fig. 3).

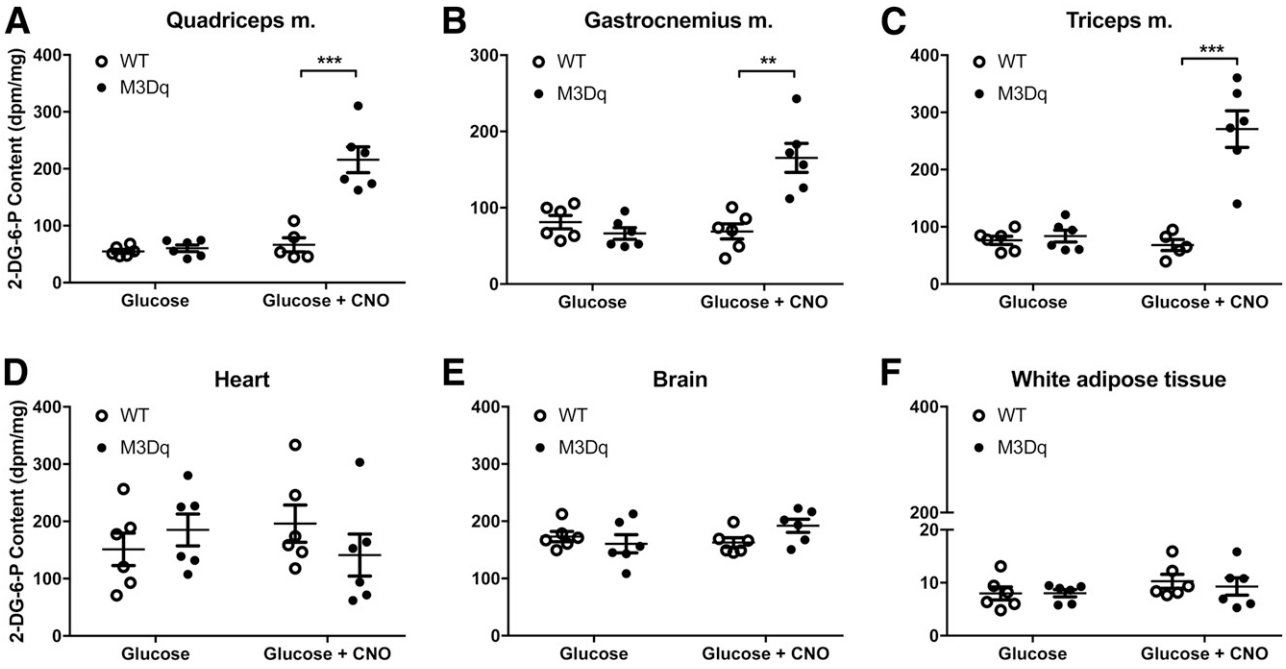

Figure 3—CNO treatment of SKM-M3Dq mice promotes selective uptake of glucose into mouse SKM in vivo. SKM-M3Dq mice (M3Dq) and WT control littermates were fasted overnight and then injected with glucose (2 mg/kg i.p.) containing 10 μCi of [1-^{14}C]2-DG, either in the presence or absence of CNO (1 mg/kg i.p.). Two hours after injections, mice were sacrificed, tissues were collected, and the [^{14}C]2-DG-6-phosphate (2-DG-6-P) content was determined (see RESEARCH DESIGN AND METHODS for details). *A–C*: SKM tissues. *D–F*: Non-SKM tissues. All experiments were carried out with male littermates that were at least 8 weeks old. Data are presented as means ± SEM (n = 5 or 6 mice/group). $^{**}P < 0.01$, $^{***}P < 0.001$ vs. WT (Student t test). m., muscle.

Moreover, CNO-treated HFD SKM-M3Dq mice showed significantly improved glucose tolerance (Fig. 5*B*) and whole-body insulin tolerance (ITT) (Fig. 5*C*), as compared with their CNO-treated HFD WT littermates. CNO treatment had no significant effect on mouse body weight (Fig. 5*A*). The beneficial metabolic effects caused by CNO treatment of the HFD SKM-M3Dq mice were not due to changes in insulin secretion, because the i.p. coinjection of glucose (2 g/kg) and CNO (1 mg/kg) caused comparable increases in insulin secretion in HFD SKM-M3Dq mice and HFD WT littermates (Supplementary Fig. 7).

Metabolic Studies With Mutant Mice Lacking $G\alpha_{q/11}$ Selectively in SKM

To further corroborate the key role of SKM $G_{q/11}$ signaling in maintaining proper glucose homeostasis, we generated mice that lacked $G\alpha_q$ selectively in SKM (genetic background: $G\alpha_{11}{}^{-/-}$) (for details, see RESEARCH DESIGN AND METHODS) (Fig. 5*D*). For the sake of simplicity, we refer to these mice as SKM-$G_{q/11}$ knockout (KO) mice. SKM-$G_{q/11}$ KO mice consuming regular chow did not differ from their control littermates ($Ga_q{}^{flox/flox}Ga_{11}{}^{-/-}$ mice) in body weight, glycemia, glucose tolerance, and whole-body insulin sensitivity (Supplementary Fig. 8). In contrast,

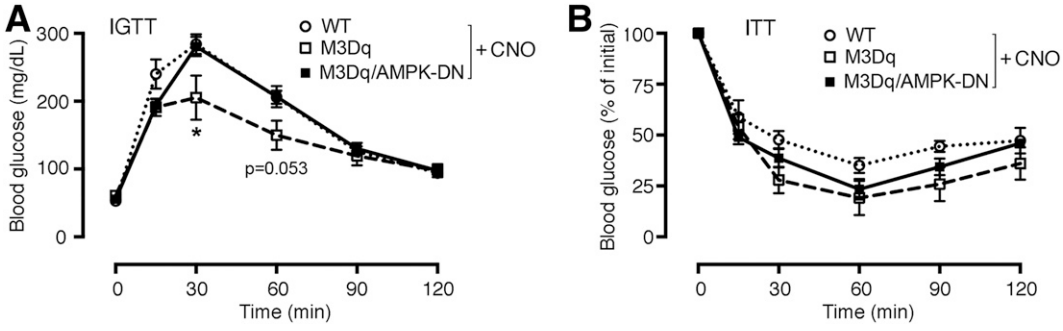

Figure 4—Metabolic studies with SKM-M3Dq mice that express a DN version of AMPK in SKM (M3Dq/AMPK-DN mice). *A*: IGTT. SKM-M3Dq mice (M3Dq), M3Dq/AMPK-DN mice, and WT control littermates were injected i.p. with glucose (2 g/kg) plus CNO (1 mg/kg). *B*: ITT. The same mice as used in *A* were injected i.p. with insulin (1.5 units/kg) plus CNO (1 mg/kg). Data are given as means ± SEM (n = 4–8 mice/group). $^{*}P < 0.05$ vs. WT (Student t test).

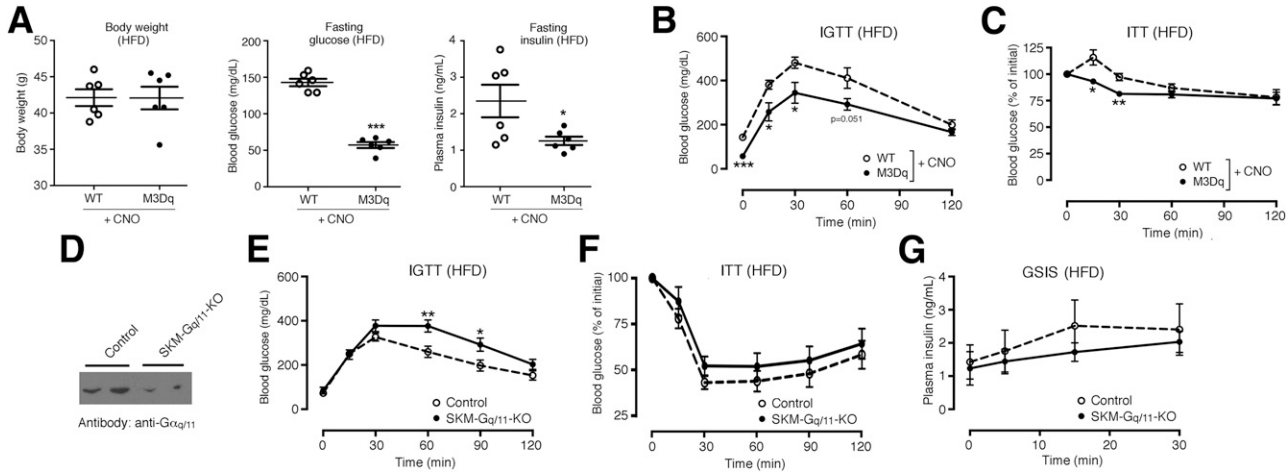

Figure 5—Metabolic studies with SKM-M3Dq transgenic and SKM-$G_{q/11}$ mutant mice maintained on an HFD. *A–C*: Metabolic studies with SKM-M3Dq mice (M3Dq) and WT control littermates maintained on an HFD for at least 8 weeks. Prior to metabolic testing, CNO (0.25 mg/mL) was added to the drinking water for 1 week. *A*: Body weight and fasting blood glucose and plasma insulin levels. *B*: IGTT. Mice were injected with glucose (2 g/kg i.p.). *C*: ITT. SKM-M3Dq mice (M3Dq) and WT control littermates were injected with insulin (0.75 units/kg i.p.). *D–G*: Generation and analysis of mice lacking $G\alpha_q$ selectively in SKM (genetic background: $G\alpha_{11}{}^{-/-}$) (SKM-$G_{q/11}$ KO mice). *D*: Representative Western blot indicating that $G\alpha_{q/11}$ expression is greatly reduced in SKM (triceps muscle) of SKM-$G_{q/11}$ KO mice (genotype: HSA-Cre(ER^{T2}) $Ga_q{}^{flox/flox}Ga_{11}{}^{-/-}$). $Ga_q{}^{flox/flox}Ga_{11}{}^{-/-}$ mice littermates that lacked the Cre(ER^{T2}) transgene served as control animals. SKM-$G_{q/11}$ KO and control littermates consumed an HFD for at least 8 weeks. *E*: IGTT. Mice were injected with glucose (2 g/kg i.p.). *F*: ITT. Mice were injected with insulin (0.75 units/kg i.p.). *G*: Glucose-stimulated insulin secretion (GSIS). Mice were treated with glucose (2 g/kg i.p.), followed by the measurement of plasma insulin levels at the indicated time points. All experiments were carried out with male littermates that were at least 16 weeks old. Data are presented as means ± SEM (6 mice per group). $^*P < 0.05$, $^{**}P < 0.01$, $^{***}P < 0.001$ vs. WT (Student *t* test).

SKM-$G_{q/11}$ KO mice that had been maintained on an HFD for at least 8 weeks displayed significantly impaired glucose tolerance (Fig. 5*E*) and showed a trend toward reduced insulin sensitivity (Fig. 5*F*), as compared with their HFD control littermates. The lack of SKM $G_{q/11}$ signaling had no significant effect on glucose-induced insulin secretion (Fig. 5*G*), body weight, and basal blood glucose and plasma insulin levels (Supplementary Fig. 9). The fact that the SKM-$G_{q/11}$ KO mice showed only a relatively mild metabolic phenotype may be because the $G_{q/11}$ KO was incomplete (Fig. 5*D*).

Receptor-Mediated Activation of G_q Signaling Also Improves Glucose Uptake in Human SKM Cells

We next wanted to explore whether receptor-mediated activation of G_q signaling also promoted glucose uptake in human SKM cells. We mined the Genotype-Tissue Expression database (33) for GPCRs that show significant changes in expression levels in SKM of patients suffering from type 2 diabetes. This analysis identified 15 GPCRs that were either up- or downregulated in diabetic SKM (Supplementary Table 1). Among the receptors that showed increased expression was the G_q-coupled OT receptor. Because of its limited expression in other tissues (34) and well-known pharmacology, we studied the function of the OT receptor in primary HSMMs. Strikingly, OT (1 μmol/L) treatment of HSMMs stimulated glucose uptake to a similar degree as insulin (100 nmol/L) (Fig. 6*A*). The combined application of OT and insulin did not lead to a further increase in glucose uptake (Fig. 6*A*).

The stimulatory actions of OT on glucose uptake could be strongly inhibited by treatment of HSMMs with L371,257 (1 μmol/L), a selective OT receptor antagonist (35,36) (Fig. 6*B*), indicative of the involvement of OT receptors. The OT-induced increase in glucose uptake could also be completely prevented by FR900359 (1 μmol/L), a selective blocker of G_q signaling (29), and by compound C (10 μmol/L), an AMPK inhibitor (Fig. 6*B*). Consistent with this latter observation, OT (1 μmol/L) treatment of HSMMs led to a time-dependent increase in AMPK phosphorylation (Fig. 6*C* and *D*).

A recent study has shown that a single intranasal dose of OT can improve insulin sensitivity in humans (37). It remains to be explored whether the OT receptor-mediated glucose uptake into SKM contributes to this beneficial OT effect. Chronic OT administration causes sustained weight reduction by reducing caloric intake and increasing energy expenditure in rodents and nonhuman primates, most likely involving central and peripheral mechanisms (38). Taken together, these studies suggest that selective, metabolically stable OT receptor agonists may prove beneficial for the treatment of type 2 diabetes and related metabolic disorders.

We also expressed the M3Dq DREADD in HSMMs by using an M3Dq-encoding adenovirus. For control purposes, we transduced HSMMs with an adenovirus coding for GFP. As observed with mouse SKM cells, CNO treatment (10 μmol/L) strongly promoted glucose uptake by M3Dq-expressing HSMMs (Fig. 6*E*), which was accompanied by a time-dependent increase in AMPK phosphorylation

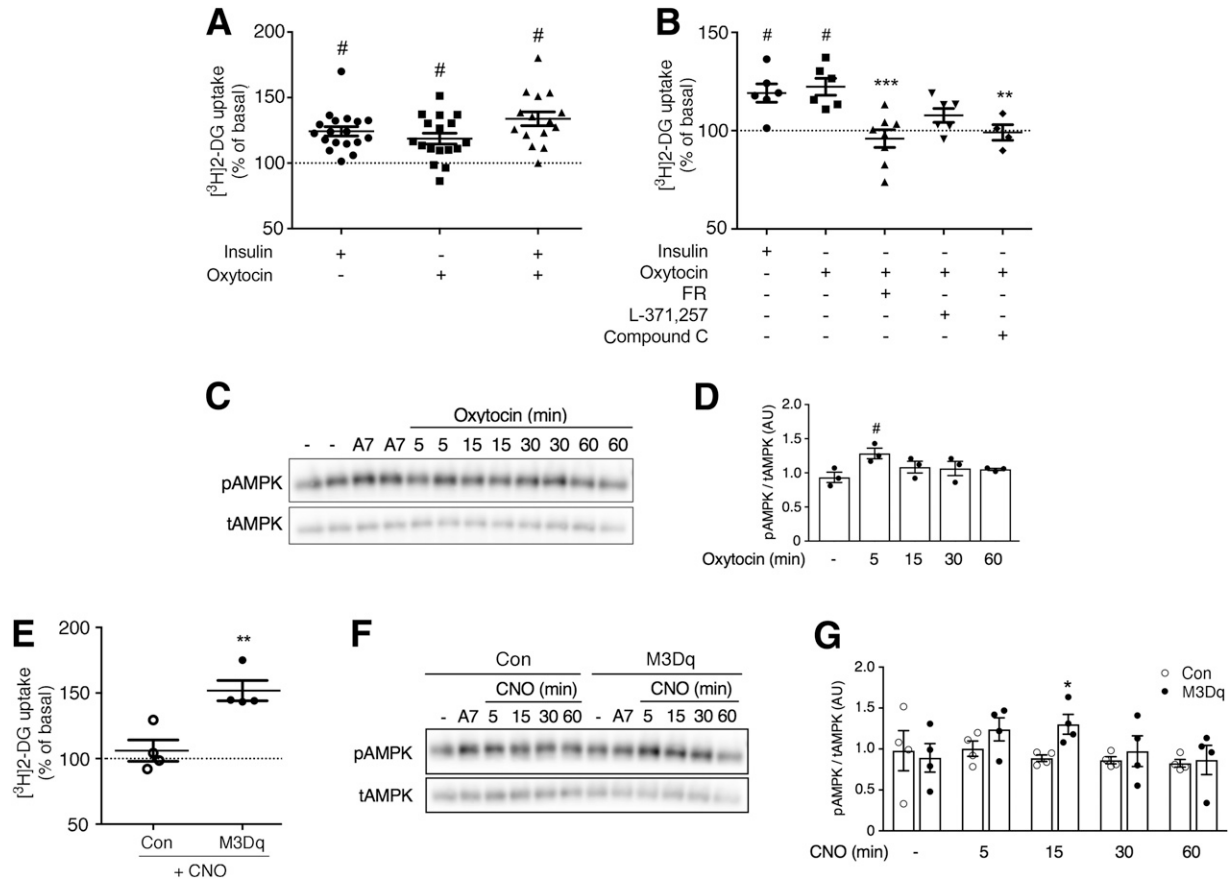

Figure 6—Glucose uptake and Western blotting studies with primary HSMMs. *A*: HSMMs were treated with insulin (100 nmol/L), OT (1 μmol/L), or a mixture of insulin (100 nmol/L) and OT (1 μmol/L) (for details, see RESEARCH DESIGN AND METHODS). Drug-induced increases in [^{3}H]2-DG uptake were determined as described in RESEARCH DESIGN AND METHODS. *B*: OT (1 μmol/L)-induced [^{3}H]2-DG uptake is abolished or greatly reduced by several pharmacological inhibitors. The following inhibitors were used: FR900359 (FR; 1 μmol/L), selective $G_{q/11}$ inhibitor; L371,257 (1 μmol/L), selective OT receptor antagonist; and compound C (10 μmol/L), AMPK blocker. *C*: Representative Western blot demonstrating that OT (1 μmol/L) treatment of HSMMs promotes AMPK phosphorylation (at 5 min). A769662 (A7; 30-min incubation; 10 μmol/L), a potent activator of AMPK, served as a positive control. *D*: Densitometric quantification of immunoblotting data shown in *C* (means ± SEM; three independent experiments; #$P < 0.05$ as compared with no drug). *E*: Activation of the G_q-linked M3Dq designer receptor promotes glucose uptake in human SKM cells. HSMMs were transduced with adenoviruses encoding either GFP (control [Con]) or M3Dq, as described in RESEARCH DESIGN AND METHODS. Transduced HSMMs were then treated with CNO (10 μmol/L), followed by [^{3}H]2-DG uptake measurements. *F*: Representative Western blot demonstrating that CNO (10 μmol/L) treatment of HSMMs expressing the M3Dq construct promotes AMPK phosphorylation. Western blotting studies were carried out with HSMMs expressing either M3Dq or GFP (control). CNO selectively promotes AMPK phosphorylation in M3Dq-expressing cells (at 15 min). *G*: Densitometric quantification of immunoblotting data shown in *F* (means ± SEM; four independent experiments; *$P < 0.05$ as compared with control). Glucose uptake data are given as means ± SEM of 15–18 (*A*) or 4–8 (*B* and *E*) independent experiments performed in duplicate. All responses were expressed relative to baseline responses (set equal to 100%) obtained in the absence of drugs. Basal [^{3}H]2-DG uptake values were not significantly different ($P = 0.60$) between M3Dq-expressing and GFP control cells (4,630 ± 1,605 and 3,442 ± 1,416 dpm/mg protein, respectively). #$P < 0.05$ as compared with baseline (100%; no drug treatment; one-sample *t* test) (*A* and *B*); **$P < 0.01$, ***$P < 0.001$ vs. OT alone (one-way ANOVA with Dunnett multiple-comparisons test) (*B*); **$P < 0.01$ vs. control (*t* test) (*E*). AU, arbitrary units; tAMPK, total AMPK.

(Fig. 6*F* and *G*). These responses were absent in CNO-treated control HSMMs (Fig. 6*E*–*G*). These observations suggest the potential usefulness of DREADD technology to improve SKM glucose uptake for therapeutic purposes by employing gene therapeutic approaches, such as virus-mediated expression of DREADDs in SKM (39).

Taken in isolation, the Western blotting data shown in Fig. 6 and Supplementary Fig. 5 are not sufficient to link AMPK phosphorylation to the observed metabolic phenotypes. However, the AMPK phosphorylation data nicely complement the in vivo metabolic data obtained with SKM M3Dq-AMPK(DN) mutant mice and the results of in vitro studies using an AMPK inhibitor, strongly implicating G_q-mediated AMPK phosphorylation in SKM in the observed beneficial metabolic effects.

Taken together, our data clearly indicate that receptor-mediated activation of G_q signaling in primary human SKM cells strongly promotes glucose uptake and that the mechanisms involved in this activity are conserved among mouse and human SKM. As discussed above, these findings are of considerable translational relevance.

Conclusions

In this study, we provide convincing evidence that receptor-mediated stimulation of SKM G_q signaling strongly promotes glucose uptake into SKM in vivo. Activation of this pathway is able to greatly ameliorate the metabolic deficits associated with the consumption of an HFD. We also show that G_q-linked SKM OT receptors can promote glucose uptake in primary human SKM cells. As a general rule, the activation of G_q-coupled receptors leads to ncreases in intracellular inositol 1,4,5-trisphosphate and calcium levels. Elevated cytoplasmic calcium levels have been shown to activate AMPK through CaMKK2-mediated phosphorylation (40). The data presented in Figs. 1*A* and *C*, 2*D*, and 6*A* strongly suggest that activation of SKM G_q signaling can promote SKM glucose uptake/GLUT4 translocation in an insulin-independent fashion, most likely mediated via stimulation of AMPK. Consistent with this observation, it has been demonstrated that activation of SKM AMPK initiates a signaling cascade that is able to stimulate GLUT4 translocation and glucose uptake in an insulin/Akt-independent fashion (41–43). Although the metabolic phenotypes displayed by the SKM-$G_{q/11}$ KO mice were relatively mild, this observation does not reduce the potential utility of engaging G_q cross talk to insulin signaling or glucose uptake in patients with metabolic disease. Because type 2 diabetes is characterized by impaired insulin receptor signaling in peripheral tissues including SKM, the development of novel drugs that can stimulate SKM G_q signaling (e.g., agonists acting on SKM G_q-coupled receptors) appears an attractive goal.

Acknowledgments. The authors thank Yinghong Cui (NIDDK, Bethesda, MD) for providing expert technical assistance, Dr. Steven Dudas for help with the FACS experiments, and Dr. Oksana Gavrilova and staff at the NIDDK Mouse Metabolism Core for carrying out the in vivo glucose uptake studies and for many valuable discussions. The authors also thank Dr. Philip Bilan and Dr. Amira Klip (University of Toronto, Toronto, Ontario, Canada) for providing the L6-GLUT4-myc cells and for helpful suggestions regarding the use of these cells. Dr. Erik Richter (University of Copenhagen, Copenhagen, Denmark) provided valuable advice throughout the course of this study. The $Ga_q^{flox/flox}Ga_{11}^{-/-}$ mice were a gift from Dr. Stefan Offermanns (Max Planck Institute, Bad Nauheim, Germany). The MCK-AMPK-DN mice were generously provided by Dr. Henriette van Praag (National Institute on Aging, Baltimore, MD), with the help of Dr. Morris Birnbaum (Pfizer, Cambridge, MA). The pHSAvpSV40pA plasmid was a gift from Dr. Jeffrey Chamberlain (University of Washington, Seattle, WA). The HA-hM3Dq-p2A-mCitrine plasmid was provided by Dr. Bryan Roth (University of North Carolina at Chapel Hill, Chapel Hill, NC). The adenovirus coding for GFP was a kind gift by Dr. Marc Montminy (Salk Institute, La Jolla, CA).

Funding. This research was funded by the Intramural Research Program of the NIDDK (to D.B.J.B., J.M., A.C., R.L., H.L., and J.W.).

Duality of Interest. No potential conflicts of interest relevant to this article were reported.

Author Contributions. D.B.J.B., J.M., and J.W. designed and conceived the experiments and wrote the manuscript. D.B.J.B., J.M., J.R.K., D.D., A.C., and R.L. performed and analyzed experiments. J.R.K. and T.E.J. designed, performed, and analyzed a series of experiments relevant to this study. H.L. generated the SKM-M3Dq mice. D.M. provided the HSA-Cre(ER^{T2}) mice and helpful advice. J.W. is the guarantor of this work and, as such, had full access to all of the data in the study and takes responsibility for the integrity of the data and the accuracy of the data analysis.

Data Availability. The datasets generated during and/or analyzed during the current study are available from the corresponding author on reasonable request.

References

1. Kahn SE, Cooper ME, Del Prato S. Pathophysiology and treatment of type 2 diabetes: perspectives on the past, present, and future. Lancet 2014;383:1068–1083
2. DeFronzo RA, Ferrannini E, Groop L, et al. Type 2 diabetes mellitus. Nat Rev Dis Primers 2015;1:15019
3. Herman MA, Kahn BB. Glucose transport and sensing in the maintenance of glucose homeostasis and metabolic harmony. J Clin Invest 2006;116:1767–1775
4. Sriram K, Insel PAG. G protein-coupled receptors as targets for approved drugs: how many targets and how many drugs? Mol Pharmacol 2018;93:251–258
5. Regard JB, Sato IT, Coughlin SR. Anatomical profiling of G protein-coupled receptor expression. Cell 2008;135:561–571
6. Hutchinson DS, Bengtsson T. AMP-activated protein kinase activation by adrenoceptors in L6 skeletal muscle cells: mediation by alpha1-adrenoceptors causing glucose uptake. Diabetes 2006;55:682–690
7. Merlin J, Evans BA, Csikasz RI, Bengtsson T, Summers RJ, Hutchinson DS. The M3-muscarinic acetylcholine receptor stimulates glucose uptake in L6 skeletal muscle cells by a CaMKK-AMPK-dependent mechanism. Cell Signal 2010;22:1104–1113
8. Horinouchi T, Hoshi A, Harada T, et al. Endothelin-1 suppresses insulin-stimulated Akt phosphorylation and glucose uptake via GPCR kinase 2 in skeletal muscle cells. Br J Pharmacol 2016;173:1018–1032
9. Wess J. Molecular basis of receptor/G-protein-coupling selectivity. Pharmacol Ther 1998;80:231–264
10. Wess J. Use of designer G protein-coupled receptors to dissect metabolic pathways. Trends Endocrinol Metab 2016;27:600–603
11. Urban DJ, Roth BL. DREADDs (designer receptors exclusively activated by designer drugs): chemogenetic tools with therapeutic utility. Annu Rev Pharmacol Toxicol 2015;55:399–417
12. Guettier JM, Gautam D, Scarselli M, et al. A chemical-genetic approach to study G protein regulation of beta cell function in vivo. Proc Natl Acad Sci U S A 2009;106:19197–19202
13. Jain S, Ruiz de Azua I, Lu H, White MF, Guettier JM, Wess J. Chronic activation of a designer G(q)-coupled receptor improves β cell function. J Clin Invest 2013;123:1750–1762
14. Li JH, Jain S, McMillin SM, et al. A novel experimental strategy to assess the metabolic effects of selective activation of a G(q)-coupled receptor in hepatocytes in vivo. Endocrinology 2013;154:3539–3551
15. Akhmedov D, Mendoza-Rodriguez MG, Rajendran K, Rossi M, Wess J, Berdeaux R. Gs-DREADD knock-in mice for tissue-specific, temporal stimulation of cyclic AMP signaling. Mol Cell Biol 2017;37;1–11
16. Rossi M, Zhu L, McMillin SM, et al. Hepatic Gi signaling regulates whole-body glucose homeostasis. J Clin Invest 2018;128:746–759
17. Klepac K, Kilić A, Gnad T, et al. The Gq signalling pathway inhibits brown and beige adipose tissue. Nat Commun 2016;7:10895
18. Armbruster BN, Li X, Pausch MH, Herlitze S, Roth BL. Evolving the lock to fit the key to create a family of G protein-coupled receptors potently activated by an inert ligand. Proc Natl Acad Sci U S A 2007;104:5163–5168
19. Crawford GE, Faulkner JA, Crosbie RH, Campbell KP, Froehner SC, Chamberlain JS. Assembly of the dystrophin-associated protein complex does not require the dystrophin COOH-terminal domain. J Cell Biol 2000;150:1399–1410
20. Mu J, Brozinick JT Jr., Valladares O, Bucan M, Birnbaum MJ. A role for AMP-activated protein kinase in contraction- and hypoxia-regulated glucose transport in skeletal muscle. Mol Cell 2001;7:1085–1094
21. Wettschureck N, Rütten H, Zywietz A, et al. Absence of pressure overload induced myocardial hypertrophy after conditional inactivation of Galphaq/Galpha11 in cardiomyocytes. Nat Med 2001;7:1236–1240

22. Schuler M, Ali F, Metzger E, Chambon P, Metzger D. Temporally controlled targeted somatic mutagenesis in skeletal muscles of the mouse. Genesis 2005;41: 165–170
23. Li YQ, Shrestha YB, Chen M, Chanturiya T, Gavrilova O, Weinstein LS. Gsα deficiency in adipose tissue improves glucose metabolism and insulin sensitivity without an effect on body weight. Proc Natl Acad Sci U S A 2016;113:446–451
24. Klip A, Ramlal T, Young DA, Holloszy JO. Insulin-induced translocation of glucose transporters in rat hindlimb muscles. FEBS Lett 1987;224:224–230
25. Ueyama A, Yaworsky KL, Wang Q, Ebina Y, Klip A. GLUT-4myc ectopic expression in L6 myoblasts generates a GLUT-4-specific pool conferring insulin sensitivity. Am J Physiol 1999;277:E572–E578
26. Huang C, Somwar R, Patel N, Niu W, Török D, Klip A. Sustained exposure of L6 myotubes to high glucose and insulin decreases insulin-stimulated GLUT4 translocation but upregulates GLUT4 activity. Diabetes 2002;51:2090–2098
27. Koshy S, Alizadeh P, Timchenko LT, Beeton C. Quantitative measurement of GLUT4 translocation to the plasma membrane by flow cytometry. J Vis Exp 2010;45:e2429
28. Funaki M, Randhawa P, Janmey PA. Separation of insulin signaling into distinct GLUT4 translocation and activation steps. Mol Cell Biol 2004;24:7567–7577
29. Schrage R, Schmitz AL, Gaffal E, et al. The experimental power of FR900359 to study Gq-regulated biological processes. Nat Commun 2015;6:10156
30. Kishi K, Yuasa T, Minami A, et al. AMP-activated protein kinase is activated by the stimulations of G(q)-coupled receptors. Biochem Biophys Res Commun 2000; 276:16–22
31. Kahn BB, Alquier T, Carling D, Hardie DG. AMP-activated protein kinase: ancient energy gauge provides clues to modern understanding of metabolism. Cell Metab 2005;1:15–25
32. Sung MM, Zordoky BN, Bujak AL, et al. AMPK deficiency in cardiac muscle results in dilated cardiomyopathy in the absence of changes in energy metabolism. Cardiovasc Res 2015;107:235–245
33. Wu C, Xu G, Tsai SA, Freed WJ, Lee CT. Transcriptional profiles of type 2 diabetes in human skeletal muscle reveal insulin resistance, metabolic defects, apoptosis, and molecular signatures of immune activation in response to infections. Biochem Biophys Res Commun 2017;482:282–288
34. Gimpl G, Fahrenholz F. The oxytocin receptor system: structure, function, and regulation. Physiol Rev 2001;81:629–683
35. Tahara A, Tsukada J, Tomura Y, et al. Pharmacologic characterization of the oxytocin receptor in human uterine smooth muscle cells. Br J Pharmacol 2000; 129:131–139
36. Williams PD, Clineschmidt BV, Erb JM, et al. 1-(1-[4-[(N-acetyl-4-piperidinyl)oxy]-2-methoxybenzoyl]piperidin-4- yl)-4H-3,1-benzoxazin-2(^{1}H)-one (L-371,257): a new, orally bioavailable, non-peptide oxytocin antagonist. J Med Chem 1995;38:4634–4636
37. Lawson EA, Marengi DA, DeSanti RL, Holmes TM, Schoenfeld DA, Tolley CJ. Oxytocin reduces caloric intake in men. Obesity (Silver Spring) 2015;23:950–956
38. Lawson EA. The effects of oxytocin on eating behaviour and metabolism in humans. Nat Rev Endocrinol 2017;13:700–709
39. Wang D, Zhong L, Nahid MA, Gao G. The potential of adeno-associated viral vectors for gene delivery to muscle tissue. Expert Opin Drug Deliv 2014;11:345–364
40. Jeon SM. Regulation and function of AMPK in physiology and diseases. Exp Mol Med 2016;48:e245
41. Zhou G, Sebhat IK, Zhang BB. AMPK activators–potential therapeutics for metabolic and other diseases. Acta Physiol (Oxf) 2009;196:175–190
42. Merrill GF, Kurth EJ, Hardie DG, Winder WW. AICA riboside increases AMP-activated protein kinase, fatty acid oxidation, and glucose uptake in rat muscle. Am J Physiol 1997;273:E1107–E1112
43. Hayashi T, Hirshman MF, Kurth EJ, Winder WW, Goodyear LJ. Evidence for 5′ AMP-activated protein kinase mediation of the effect of muscle contraction on glucose transport. Diabetes 1998;47:1369–1373